OPTIMAL DESIGN OF DIPOLE ANTENNAS BACKED BY A FINITE HIGH-IMPEDANCE SCREEN

G. Bianconi, F. Costa, S. Genovesi, and A. Monorchio

Dipartimento di Ingegneria dell' Informazione
Università di Pisa, Via G. Caruso 16, Pisa 56122, Italy

Abstract—The performance of a short dipole antenna closely located above a finite High-Impedance Surface (HIS) is addressed. The antenna behavior is thoroughly analyzed in the frequency range up to the HIS resonance within the region where the propagation of the TE surface waves is not allowed. In the first part of the paper the analysis of a dipole antenna above a grounded dielectric slab is considered, and then it is extended to the case of a substrate with a frequency selective surface printed on it. For all configurations, the radiation pattern of the structure and Front-to-Back Ratio (FBR) are reported and compared. It is shown that the presence of a suitable frequency selective surface, regardless of the shape of the periodic elements, guarantees the antenna matching but does not influence the behavior of the radiation patterns and the front-to-back ratio in the frequency range where only TM modes are allowed to propagate. The front-to-back ratio has been found to be maximum when the size of the generic HIS is around $0.8\lambda_g$ (where λ_g is the TM guided surface wave wavelength). All the speculations are supported by simulated and measured results.

1. INTRODUCTION

The publication of the first paper dealing with High-Impedance Surfaces (HISs) in 1999 [1] has opened a new research trend in antenna field. Indeed, since that year, the HIS surfaces have been frequently employed as a backing plane for an horizontal wire dipole to enhance the radiation efficiency of such low-profile structure [2–7]. The HISs are also currently suggested to improve the performance of other radiation devices [8–10]. In the case of the wire dipole, the interaction between the antenna and the high-impedance surface excites complex waves and

generates different resonant phenomena that require a careful analysis. The physical properties of a HIS have been rigorously studied in the case of plane wave incident on an infinite structure [11–17]. In the horizontal wire dipole case, homogenized models can be employed to predict the reflection phase of the surface both for normal and oblique incidence [13]. The model is also of vital importance for understanding the propagation mechanisms of the surface waves supported at the interface between the complex surface and the free space [15]. Some attempts to analyze the radiative behavior of a dipole antenna on a HIS by using simplified models have been done with different degrees of accuracy [18–20]. However, simple homogenized techniques cannot guarantee a good approximation of the structure when they are applied to finite models. The homogenized approach, if applied in its rigorous formulation, is adequate only in approximating the near field of infinite structures [21]. The reason of these inaccuracies is due to the propagation of surface waves on the screen and their edge diffraction, which generates additional resonances, not present in the infinite model.

The influence of the backing plane dimension on the radiation properties of the antenna is therefore of crucial importance and the actual relation between the radiation pattern of the antenna and the size of the high-impedance surface has not yet been sufficiently investigated. This aspect will be addressed in the present paper in order to determine if the increase of the HIS extension leads to an improvement of the radiation performance or if its dimension can be kept small as it is desirable for a low-profile device. First of all, the problem will be addressed in the case of a dipole antenna on the top of a grounded dielectric slab only in order to show that, in the TM (Transverse Magnetic) surface wave frequency range (before of the HIS resonance), the shape of the radiation patterns is related to the size of the structure. Then, the introduction of a Frequency Selective Surface (FSS) printed on the grounded dielectric will be taken into account. The presence of the FSS determines a HIS resonance which provides the antenna matching but causes the onset of TE (Transverse Electric) surface waves after the HIS resonance. The occurrence of TE surface waves introduces additional resonances and deteriorates the radiation patterns but their effect can be kept out of the antenna operating band. To investigate this aspect, an analysis of the dipole on the HIS has been carried out by changing the overall dimension of the screen as well as by using different unit cell shapes.

The analysis of the low-profile antenna is also supported by experimental validations on ad-hoc prototypes. The experimental tests allow both to assess the accuracy of the simulated results and

to provide the validation of the presented speculations. The paper is organized as follows: in the next section the analysis of a short dipole antenna on the top of grounded dielectric slabs with different characteristics is addressed; Section 3 shows the effect of the FSS unit cell on the radiation pattern of the antenna in the TM surface wave zone; Section 4 deals with the experimental verification of the presented theories while Section 5 suggests criteria for the optimal design of low-profile antennas. Finally, conclusions are drawn which summarize the main contributions of this work.

2. DIPOLE ON GROUNDED DIELECTRIC

In order to prove that the radiation properties of a low-profile antenna are deeply related to the ground plane size within the TM surface wave range (frequency range where the only propagating mode is the TM_0), the interaction between a short dipole antenna and a square grounded dielectric slab has been investigated. A sketch of the analyzed structure is reported in Fig. 1.

The relative dielectric constant and thickness of the employed grounded substrate are chosen to be 10 and 3.18 mm respectively. The length D of the non-resonating dipole antenna is equal to 24 mm. The distance between the antenna and the top face of the grounded dielectric surface h is fixed to 1.0 mm. The gap is considered in order to maintain the same setup of the next case in which the FSS is printed on the top of the grounded slab. However its influence is weak and the results are still valid if the dipole is etched on the dielectric interface. The antenna radiation patterns have been analyzed varying the physical and geometrical properties of the grounded dielectric slab. The frequency considered for the analysis is 4.25 GHz which corresponds to the best return loss when the FSS is placed on the grounded dielectric. To prove that the selected frequency belongs to a frequency range where only the TM_0 mode is allowed to propagate, the dispersion diagram for the dielectric slab is reported in Fig. 2. In Fig. 3 and Fig. 4 the antenna radiation patterns on E and H plane for L equal to 35 mm, 55 mm and 75 mm are reported.

The low-profile antenna radiates with a low back radiation as desired for L equal to 55 mm. This configuration allows to obtain a FBR of 25 dB and a smooth shape of the main lobe in the broadside direction. Conversely, when the ground plane dimension is increased, the antenna is characterized by a worse performance in terms of back radiation. The antenna FBR behavior is then further analyzed as a function of the grounded dielectric size for different values of the substrate thickness (Fig. 5) and relative dielectric permittivity (Fig. 6).

As it is apparent from Figs. 5 and 6 the antenna pattern is
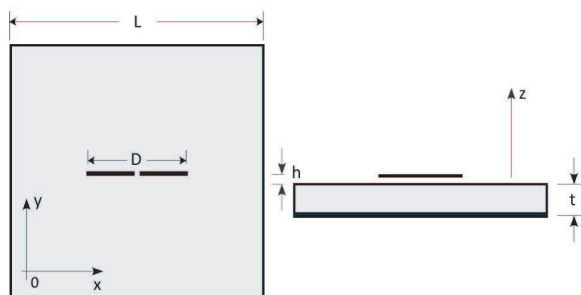
Figure 1. Geometry of the dipole antenna over the grounded dielectric slab.
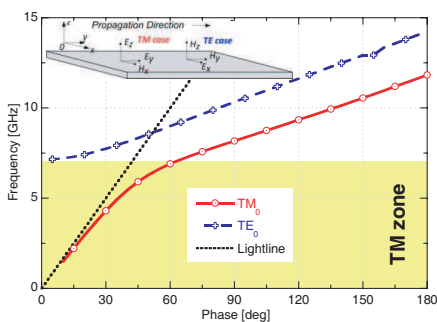
Figure 2. Dispersion diagram of the grounded dielectric slab with relative dielectric constant equal to 10 and thickness 3.18 mm.
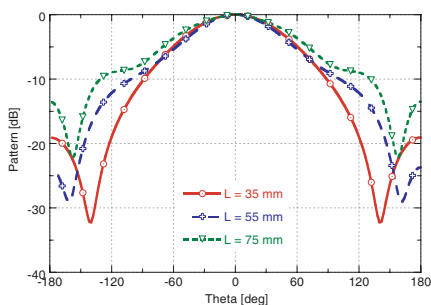
Figure 3. Antenna radiation patterns on the E-plane for different size L of the finite ground plane ($L = 35$ mm, $L = 55$ mm and $L = 75$ mm).
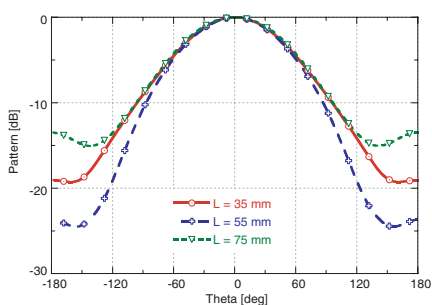
Figure 4. Antenna radiation patterns on the H-plane for different size L of the finite ground plane ($L = 35$ mm, $L = 55$ mm and $L = 75$ mm).
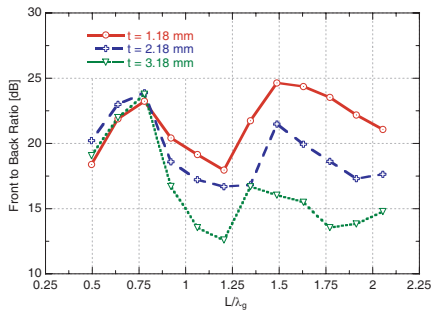
Figure 5. Comparison of antenna FBR performance at 4.25 GHz for different values of the dielectric thickness by changing the grounded substrate edge length L while maintaining constant the permittivity ($\varepsilon_r = 10$).
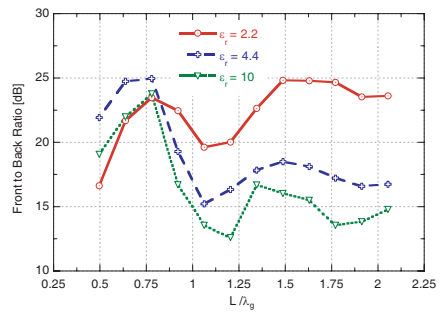
Figure 6. Comparison of antenna FBR performance at 4.25 GHz for different values of the permittivity constant of the dielectric substrate by changing the edge length L of grounded substrate while reserving the thickness ($t = 3.18$ mm).

characterized by a maximum of the FBR for $L = 0.8\lambda_g$ where λ_g is the TM$_0$ surface wave guided wavelength. The non monotonic behavior is also observed in other kinds of low profile devices [22–24] where the ground plane size strongly affects the directivity which, rather than increasing uniformly, reveals a more complex dependence. Moreover, in the case of a PIFA [25] and a patch [26] antenna with a ground plane of finite size an optimal dimension in terms of front-to-back ratio and gain has been found to be around $0.8\lambda_g$. The FBR value is strongly influenced by the dielectric relative constant and thickness of the slab when L exceeds λ_g where it oscillates before stabilizing around a constant value which depends on ε_r and t. The antenna presents the same electromagnetic behavior varying the operating frequency but the numerical results are not included in the paper for the sake of brevity.

3. DIPOLE ON HIGH-IMPEDANCE SURFACE — EFFECT OF FSS

In this section, the effect of a FSS printed on the grounded substrate is considered. In particular, the influence of the FSS unit cell shape on the FBR performance of the radiating device has been investigated in the case of frequency selective surfaces comprising patch elements and another one with Jerusalem crosses [27]. The unit cells of the mentioned FSS screens are reported in the inset of Fig. 7. The dielectric

substrate employed in the design is the Taconic CER10 ($\varepsilon_r = 10$) with a thickness of 3.18 mm. The periodicity T of the FSS screens is equal to 5.0 mm and they are both designed to allow the matching of the short dipole at 4.25 GHz. The phase of the high-impedance screen is reported in Fig. 7 when the infinite structure is illuminated by a normal incident plane wave.

The zero-phase reflection, which satisfies the so called AMC (Artificial Magnetic Conductor) condition, falls around 4.8 GHz for both the unit cell elements. In Fig. 8, the dispersion diagrams of the HISs formed by the two different FSS elements are reported. As it is evident from the two diagrams, the main resonance frequency of the antenna, which has chosen to be around 4.25 GHz, falls within the so
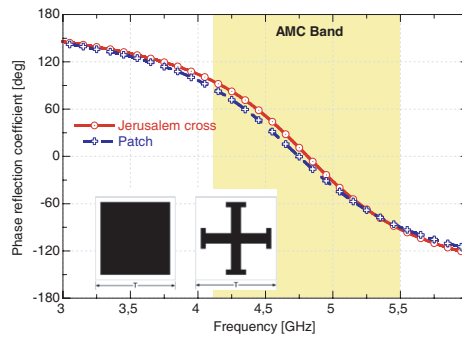
Figure 7. Phase reflection coefficient of the infinite HIS at normal incident for the two unit cells represent in the inset.
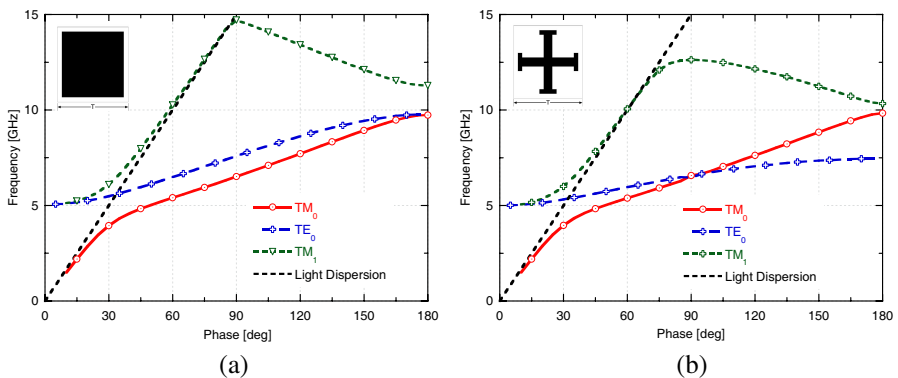
Figure 8. Dispersion diagram of the (a) patch-type and (b) Jerusalem cross type FSS elements printed on top of a 3.18 mm CER 10 grounded slab.

called TM zone. In Fig. 9 the S_{11} of the dipole antenna on the top of the patch type HIS for three different screen dimensions L is reported. The size of the HIS backing plane L is due to the number of unit cells plus an extra border of 2.5 mm that is used at the manufacturing stage to fix the antenna on the HIS. It is apparent that the dimension of the reactive ground plane does not affect the occurrence of the first minimum of the S_{11}.

Even for a larger size of the panel the first antenna resonance is exhibited at 4.25 GHz while the second one, which is much more
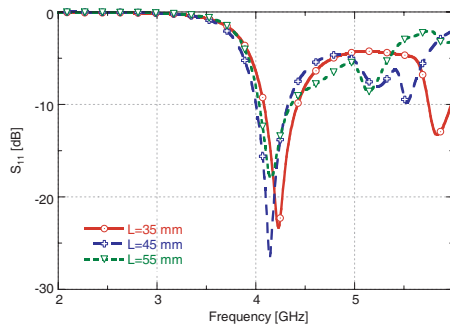
Figure 9. Reflection coefficient of the dipole antenna placed above a HIS formed by an array of patches printed on top of a grounded 3.18 mm thick CER 10 substrate. The size of the panel is varied from 35 mm (6 unit cells) to 55 mm (10 unit cells).
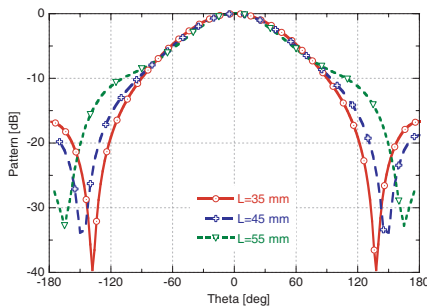
Figure 10. E-plane cut of the radiation pattern at 4.25 GHz for the dipole antenna closely placed on the patch type screen for $L = $ 35 mm, $L = $ 55 mm and $L = $ 75 mm.
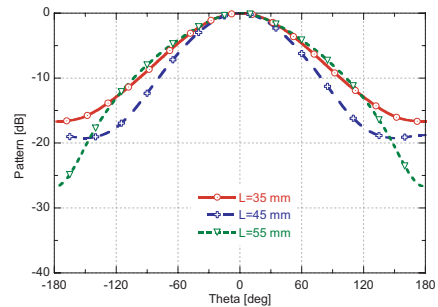
Figure 11. H-plane cut of the radiation pattern at 4.25 GHz for the dipole antenna closely placed on the patch type screen for $L = $ 35 mm, $L = $ 55 mm and $L = $ 75 mm.

dependent on the overall screen length, decreases. As expected, the dipole antenna is matched close to the frequency where the AMC resonance occurs. In Fig. 10 and Fig. 11 the radiation patterns of the dipole antenna on the top of the patch type HIS are reported on E and H planes as a function of the ground plane dimension. By observing the radiation patterns, it can be noticed that the behavior of the back radiation is non-monotonic and it is characterized by a maximum as in the case of the dipole above the grounded dielectric slab. The level of the back radiation decreases down to a value of -27.5 dB as the overall dimension L increases up to 55 mm (10 unit cells) but a further increase of L determines a worse level of the back radiation as for instance -15 dB for $L = 65$ mm (12 unit cells).

The same analysis has been performed for the case of the Jerusalem Cross screen. The results for the two structures are compared in Fig. 12 where the FBR is reported as a function of the overall HIS size L normalized to the TM_0 surface wave guided wavelength. It is interesting to notice the similar behavior of the two curves which refers to two different unit cells. They exhibit the same maximum of the FBR which takes place at $L = 0.8\lambda_g$ as in the case of the grounded dielectric slab (Fig. 5 and Fig. 6).
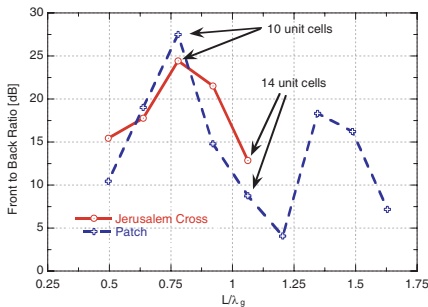
Figure 12. Comparison between the antenna FBR obtained at 4.25 GHz for the FSS comprising patch elements and the one formed by Jerusalem Cross unit cells. They are both printed on a grounded dielectric slab ($\varepsilon_r = 10$) 3.18 mm thick.
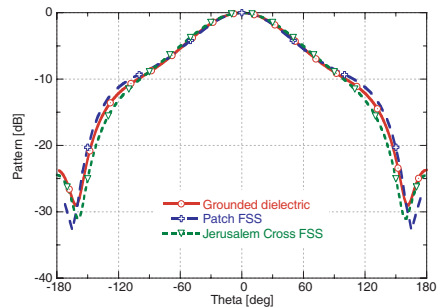
Figure 13. Comparison between the E-plane radiation pattern at 4.25 GHz for the case of a dipole above the grounded slab, a dipole on the HIS formed by the patch FSS and by Jerusalem Cross unit cells. The size of the finite panel is 55 mm.

From these results we can infer that the FSS printed on the dielectric slab is useful for achieving the antenna matching but does not strongly affect the FBR performance if the antenna is operating within the TM surface wave range. The small differences between

the two curves in Fig. 12 can be probably ascribed to the presence of the surface wave currents guided from the periodic printed surfaces even within the TM zone [28–30]. This contribution can be anyway considered of a higher order with respect to main ones (TM_0 surface wave guided by the grounded dielectric and the space wave). Such speculations can be easily proved by comparing the radiation pattern of the antenna structure in the case of a bare grounded dielectric slab or with the FSS printed on the substrate. In Fig. 13 the E-plane radiation pattern of the antenna with and without the loading FSS are reported for the optimal dimension of the backing screen, namely 55 mm.

4. EXPERIMENTAL VERIFICATION

In order to verify the proposed design methodology and the concepts introduced in the first part of the paper, some ad-hoc prototypes have been manufactured and measured. The main purpose of the tests is to verify the behavior of the FBR as a function of the structure dimension. Since it is quite troublesome to manufacture many different prototypes comprising a different number of unit cells, we recur to a different strategy. In order to motivate our procedure, let us focus on the excitation mechanism of the surface wave modes on the high-impedance surface. It is well known that only the first TM mode is supported by the structure from zero to the HIS resonance frequency. Therefore, the FBR of an antenna on the top of a high-impedance structure up to the HIS resonance is influenced by the behavior of the TM_0 surface waves only. Our approach consists on choosing a large HIS structure thus allowing to derive the FBR as a function of different electrical dimensions of the HIS by only changing the wavelength of interest within the frequency range where only the TM_0 mode is propagating. In this way, we can recover the same information on the FBR behavior as a function of the finite ground plane size by just performing measurements of the radiation patterns within the aforementioned frequency region. The procedure has been applied to two different high-impedance surfaces composed by different FSS unit cells (i.e., patch and cross). The manufactured prototypes are shown in Fig. 14.

The measured FBR as function of the HIS dimension normalized to the guided wavelength is reported in Fig. 15 both for the patch and the cross type periodic surfaces. It is evident that the measured results reveal the same behavior obtained with the simulations by increasing step by step its size.
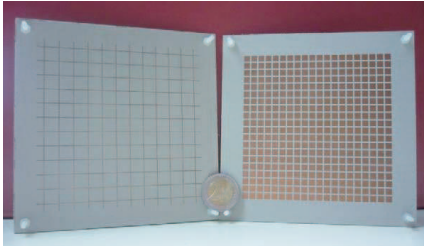
Figure 14. Large high-impedance ground planes realized for measurements ($13\,\text{cm} \times 13\,\text{cm}$). A short bow tie antenna is placed above each one and fixed by using some plexiglass screws.
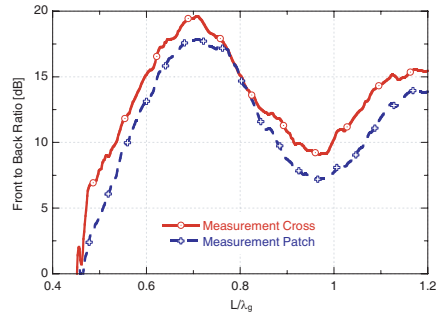
Figure 15. FBR of a dipole antenna backed by a HIS reflector as function of the panel size normalized to the operating guided wavelength.

5. OPTIMAL DESIGN OF AN HIS BASED ANTENNA

Based on the previous observations, an optimal configuration of a dipole antenna backed by a high-impedance surface has been manufactured and tested.

The HIS is composed by a 8×8 patch array, with a period of $5\,\text{mm}$ and a gap between the adjacent elements of $1\,\text{mm}$, printed on a Taconic CER10 grounded substrate with a thickness of $3.18\,\text{mm}$. The total size of the HIS panel is $0.75\lambda_g$ at the resonance which is close to the optimal size derived in the present paper. A picture of the manufactured prototype is reported in Fig. 16. The antenna above the HIS is a short bow-tie dipole printed on a FR4 thin slab $0.8\,\text{mm}$ thick. The antenna in free space is matched between $6\,\text{GHz}$ to $7\,\text{GHz}$, which is out of the band under investigation. It is worth to remark that, in order to evaluate the effect of the HIS, the feeding dipole should not be resonant in the same band of the HIS. By using a longer dipole an additional resonance can be introduced also before the HIS resonance [31]. The S_{11} of the proposed radiating device is reported in Fig. 17. When the antenna is placed above the HIS structure a wide matching is achieved because of the HIS loading.

The first minimum of the S_{11} is due to the HIS resonance and the subsequent ones are introduced by the propagation of TE surface waves on the finite HIS structure. By keeping the panel size as small as possible, the additional TE resonances can be placed far from the first one with a consequent enlargement of the bandwidth. It is therefore
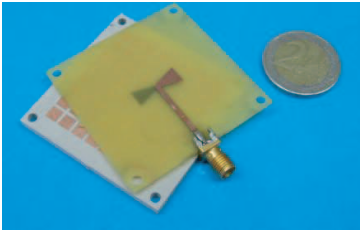
Figure 16. A picture of the optimal antenna design.
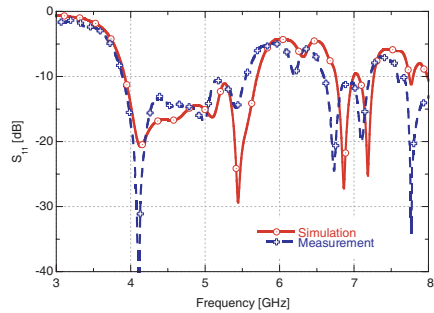
Figure 17. Measured and simulated S_{11} of the antenna shown in Fig. 16.
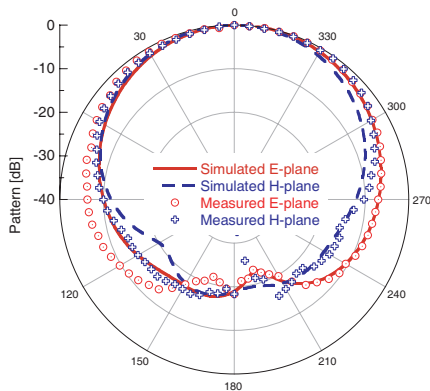
Figure 18. Measured and simulated patterns on E and H plane at 4.0 GHz.
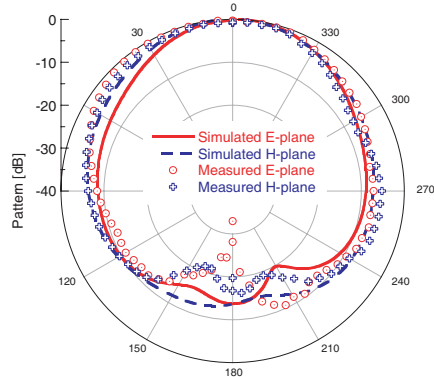
Figure 19. Measured and simulated patterns on E and H plane at 4.5 GHz.

important to underline that if the dimension of the HIS panel were further increased with respect to the optimal dimension a twofold drawback would be obtained: a worsening of the patterns within the TM band of the HIS as here demonstrated and a bandwidth reduction due to the onset of the TE resonance before 5 GHz. After the onset of the first TE surface wave resonance, the radiation patterns of the antenna are not broadside anymore. In Fig. 18 to Fig. 20 the radiation patterns of the antenna are shown at 4.0 GHz, 4.5 GHz and 5.0 GHz. The patterns are characterized by a low back radiation according to our speculations. The operating bandwidth of the antenna is more than 1.0 GHz extending up to 5.0 GHz and the radiation patterns are almost symmetric.
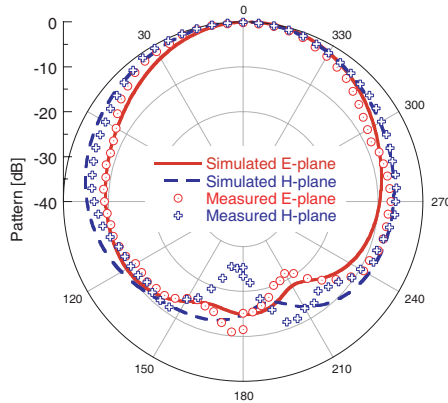
Figure 20. Measured and simulated patterns on E and H plane at 5.0 GHz.

6. CONCLUSION

The observation of the radiation properties of a short dipole antenna placed close to a HIS has provided the evidence of a correlation between the finite dimension of the backing screen and the non-monotonic behaviour of the front-to-back ratio. The optimal FBR has been found for a dimension of the screen around $0.8\lambda_g$, with a good agreement between the estimates provided by simulations and data collected with measurements on realized prototypes. The employment of printed FSS on low-profile antenna design has been found useful to guarantee the matching of a non-resonant device placed above the HIS but it has resulted negligible with respect to the level of FBR in the TM surface wave band.

REFERENCES

1. Sievenpiper, D., L. Zhang, R. F. J. Broas, N. G. Alexopolous, and E. Yablonovitch, "High-impedance electromagnetic surfaces with forbidden frequency band," *IEEE Trans. Microwave Theory Tech.*, Vol. 47, No. 11, 2059–2074, Nov. 1999.

2. Yang, F. and Y. Rahmat-Samii, "Reflection phase characterizations of the EBG ground plane for low profile wire antenna applications," *IEEE Trans. Antennas Propag.*, Vol. 51, No. 10, 2691–2703, October 2003.

3. Baracco, J.-M., L. Salghetti-Drioli, and P. de Maagt, "AMC low profile wideband reference antenna for GPS and GALILEO

systems," *IEEE Trans. Antennas Propag.*, Vol. 56, No. 8, 2540–2547, 2008.

4. Akhoondzadeh-Asl, L., D. J. Kern, P. S. Hall, and D. H. Werner, "Wideband dipoles on electromagnetic bandgap ground planes," *IEEE Trans. Antennas Propag.*, Vol. 55, No. 9, 2426–2434, 2007.

5. Elek, F., R. Abhari, and G. V. Eleftheriades, "A uni-directional ring-slot antenna achieved by using an electromagnetic band-gap surface," *IEEE Trans. Antennas Propag.,* Vol. 53, No. 1, 181–190, 2005.

6. Costa, F., A. Monorchio, S. Talarico, and F. M. Valeri, "An active high impedance surface for low profile tunable and steerable antennas," *IEEE Antennas Wireless Propag. Lett*, Vol. 7, 676–680, 2008.

7. Best, S. and D. Hanna, "Design of a broadband dipole in close proximity to an EBG ground plane," *IEEE Antennas and Propagation Magazine*, Vol. 50, No. 6, 52–64, 2008.

8. Tran, C.-M., H. Hafdallah-Ouslimani, L. Zhou, A. C. Priou, H. Teillet, J.-Y. Daden, and A. Ourir, "High impedance surfaces based antennas for high data rate communications at 40 GHz," *Progress In Electromagnetics Research C*, Vol. 13, 217–229, 2010.

9. Bao, X. L., G. Ruvio, and M. J. Amman, "Directional dual-band slot antenna with dual-bandgap high-impedance-surface reflector," *Progress In Electromagnetics Research C*, Vol. 9, 1–11, 2009.

10. Rajo-Iglesias, E., L. Inclan-Sanchez, and O. Quevedo-Teruel, "Back radiation reduction in patch antennas using planar soft surfaces," *Progress In Electromagnetics Research Letters*, Vol. 6, 123–130, 2009.

11. Tretyakov, S., *Analytical Modelling in Applied Electromagnetics*, Artech House, Boston, 2003.

12. Clavijo, S., R. E. Dıaz, and W. E. McKinzie, III, "Desing methodology for Sievenpiper high-impedance surfaces: An artificial magnetic conductor for positive gain electrically small antennas," *IEEE Trans. Antennas Propag.*, Vol. 51, No. 10, 2678–2690, October 2003.

13. Luukkonen, O., C. Simovski, G. Granet, G. Goussetis, D. Lioubtchenko, A. V. Räisänen, and S. A. Tretyakov, "Simple and accurate analytical model of planar grids and high-impedance surfaces comprising metal strips or patches," *IEEE Trans. Antennas Propag.*, Vol. 56, No. 6, 1624–1632, 2008.

14. Kern, D. J., D. H. Werner, A. Monorchio, L. Lanuzza, and

M. J. Wilhelm, "The design synthesis of multiband artificial magnetic conductors using high impedance frequency selective surfaces," *IEEE Trans. Antennas Propag.*, Vol. 53, No. 1, Part 1, 8–17, January 2005.

15. Maci, S. and A. Cucini, "FSS-based EBG surfaces," *Electromagnetic Metamaterials: Physics and Engineering Aspects*, N. Engheta and R. W. Ziolkowski (eds.), Wiley-Interscience, New York, 2006.

16. Yakovlev, A. B., O. Luukkonen, C. R. Simovski, S. A. Tretyakov, S. Paulotto, P. Baccarelli, and G. W. Hanson, "Analytical modeling of surface waves on high impedance surfaces," *Metamaterials and Plasmonics: Fundamentals, Modelling, Applications*, S. Zouhdi, A. Sihvola, and A. P. Vinogradov (eds.), 239–254, NATO Science for Peace and Security Series B, 2009.

17. O. Luukkonen, C. R. Simovski, and S. A. Tretyakov, "Grounded uniaxial material slabs as magnetic conductors," *Progress In Electromagnetics Research B*, Vol. 15, 267–283, 2009.

18. Hansen, R. C., "Effects of a high-impedance screen on a dipole antenna," *IEEE Antennas Wireless Propag. Lett.*, Vol. 1, 46–49, 2002.

19. Abedin, M. F. and M. Ali, "Effects of EBG reflection phase profiles on the input impedance and bandwidth of ultra-thin directional dipoles," *IEEE Trans. Antennas Propag.*, Vol. 53, No. 11, 3664–3672, 2005.

20. Tretyakov, S. A. and C. R. Simovski, "Wire antennas near artificial impedance surfaces," *Microwave and Optical Technology Letters*, Vol. 27, No. 1, 46–50, 2000.

21. Paulotto, S., P. Baccarelli, P. Burghignoli, G. Lovat, G. Hanson, and A. B. Yakovlev, "Homogenized Green's functions for an aperiodic line source over planar densely periodic artificial impedance surfaces," *IEEE Trans. on Microwave Theory and Techniques*, Vol. 58, No. 7, 1807–1817, July 2010.

22. Moosavi, P. and L. Shafai, "Directivity of microstrip ring antennas and effects of finite ground plane on the radiation parameters," *IEEE Antennas and Propagation Society International Symposium*, Vol. 2, 672–675, June 1998.

23. Marg, R., I. Schon, and A. F. Jacob, "Finite ground plane effects on the radiation pattern of small microstrip arras," *IEE Proc. Microw. Antennas Propag.*, Vol. 147, No. 2, 139–143, April 2000.

24. Namiki, T., Y. Murayama, and K. Ito, "Improving radiation-pattern distorsion of a patch antenna having a finite ground plane," *IEEE Trans. Antennas Propag.*, Vol. 51, No. 3, March

2003.

25. Huynh, M.-C. and W. Stutzman, "Ground plane effects on planar inverted-F antenna (PIFA) performance," *IEE Proc. Microw. Antennas Propag.*, Vol. 150, No. 4, 209–213, August 2003.

26. Kim, T.-Y., J.-W. Park, and B.-G. Kim, "Impact of a square grounded dielectric substrate on the radiation characteristics of a rectangular microstrip patch antenna," *IEEE Antennas and Propagation Society International Symposium, 2009. APSURSI'09*, 1–4, June 1–5, 2009.

27. Munk, B. A., *Frequency Selective Surfaces — Theory and Design*, John Wiley & Sons, New York, 2000.

28. Munk, B. A., D. S. Janning, J. B. Pryor, and R. J. Marhefka, "Scattering from surface waves on finite FSS," *IEEE Trans. Antennas Propag.*, Vol. 49, 1782–1793, December 2001.

29. Janning, D. S. and B. A. Munk, "Effects of surface waves on the currents of truncated periodic arrays," *IEEE Trans. on Antennas and Propagation*, Vol. 50, No. 9, 1254–1265, 2002.

30. Çivi, Ö. A. and P. H. Pathak, "Array guided surface waves on a finite planar array of dipoles with or without a grounded substrate," *IEEE Trans. Antennas Propag.*, Vol. 54, No. 8, 2244–2252, August 2006.

31. Azad, M. Z. and M. Ali, "Novel wideband directional dipole antenna on a mushroom like EBG structure," *IEEE Trans. Antennas Propag.*, Vol. 56, No. 5, 1242–1250, 2008.